Research Article | Vol. 11, No. 10 / 1 October 2020 / Biomedical Optics Express 5603
Biomedical Optics EXPRESS

Vision with pulsed infrared light is mediated by nonlinear optical processes

SILVESTRE MANZANERA, DANIEL SOLA, NOE KHALIFA, AND PABLO ARTAL*

Laboratorio de Óptica, Instituto Universitario de Investigación en Óptica y Nanofísica, Universidad de Murcia, Campus de Espinardo (Edificio 34), E-30100 Murcia, Spain
pablo@um.es

Abstract: When the eye is exposed to pulsed infrared (IR) light, it is perceived as visible of the corresponding half wavelength. Previous studies have reported evidence that this is due to a non-linear two-photon absorption process. We have carried out a study which provides additional support to this nonlinear hypothesis. To this end, we have measured the spectral sensitivity at 2 different pulse repetition rates and have developed a theoretical model to account for the experimental observations. This model predicts a ratio between the minimum powers needed to detect the visual stimulus at the 2 pulse repetition rates employed of 0.45 if the stimulus were detected through a nonlinear effect and 1 if it were caused by a linear effect as in normal vision. The value experimentally found was 0.52 ± 0.07, which supports the hypothesis of a nonlinear origin of the two-photon vision phenomena.

1. Introduction

In humans, the eye is only sensitive to a narrow band of the electromagnetic spectrum. The CIE established in 1924 [1] the standard spectral sensitivity of the average human observer under photopic luminous conditions. The maximum visual sensitivity occurs approximately at 555 nm and rapidly declines towards both shorter and longer wavelengths, and we assume that our ability to perceive radiation is limited to the range from 400 to 700 nm in what is called the *visible* part of the spectrum.

This does not mean a complete lack of sensitivity to longer wavelengths in the near infrared (IR), perceived as a pale red. Some authors had investigated this issue many decades ago, for instance, Goodeve [2] in 1936 or Griffin and colleagues [3] in 1947. The latter reported that the sensitivity of the peripheral retina at 1050 nm is 3×10^{-13} times the value at 505 nm. In consequence this small factor greatly reduces, in practice, our ability to detect IR light.

With the advent of new light sources and, in particular, pulsed lasers, a new visual phenomenon was discovered. The first known report was from Vasilenko et al. [4] who in their paper of 1965 claimed that, when using a pulsed laser, different observers perceived IR radiation as visible light corresponding to half the wavelength of the IR. These authors estimated the wavelength of the visible light that would have produced the same color perception (perceived wavelength) and suggested that the second harmonic of the IR radiation was responsible for these observations. After this result, it was thought that either the cornea or some other tissue in the retina were acting as a nonlinear media allowing the two photons interaction and emitting one with half the wavelength (second harmonic), which was then sensed by the retina. Some other studies based on psychophysical experiments followed. Sliney and colleagues [5] measured the minimum average power at the cornea, or power threshold, required to elicit this sensation and found a deviation from Bloch's law [6,7] which they attributed to a nonlinear effect and in particular also suggesting the second harmonic generation (SHG) process as responsible. Some other authors [8] also supported this theory.

#403695 https://doi.org/10.1364/BOE.403695
Journal © 2020 Received 24 Jul 2020; revised 7 Sep 2020; accepted 9 Sep 2020; published 15 Sep 2020

Biomedical Optics EXPRESS

However, Dmitriev et al. [9] proposed a different nonlinear mechanism to explain this phenomenon. They measured both the perceived wavelength and the power thresholds and concluded that the most plausible explanation for this color perception in the IR was a two-photon (2P) photoisomerization of the visual pigment. The opsin, the light sensitive molecule in the cones, was activated by the simultaneous absorption of 2 IR photons which were then interpreted by the visual system as the absorption of one single visible photon. Palczewska et al. [10] supported this theory by combining psychophysical with biochemical and electrophysiological experiments. The psychophysical experiments they carried out included the estimation of the perceived wavelength and the power thresholds at several wavelengths using two different pulse widths in two subjects. The fact that the power thresholds were lower with the shorter pulses was an indication of the nonlinear nature of the studied mechanism. Similar findings were also reported by Ruminski et al. [11] after testing different locations in the retina with IR light with 2 different pulse widths.

All the above referenced studies have shown experimental evidence pointing to the involvement of a nonlinear optical effect in this visual mechanism. However, we believe it is possible to create a more detailed theoretical framework to describe the interactions of the IR photons on the retina and account for the observations. The purpose of this work is to carry out a comprehensive study able to provide further proof of the involvement of a nonlinear process, consisting of a psychophysical experiment with sufficient number of observers and supported by a theoretical model. To this end we devised a new experiment based on measurements of the power thresholds at different pulse repetition rates. The theoretical model we propose shows that the comparison of these power thresholds at the different pulse repetition rates is highly dependent on the number of photons (1 or 2) involved in the process. The comparison between the expected and experimental results will allow us to provide additional support to the hypothesis of a nonlinear process and the involvement of a 2P process.

2. Methods

2.1. Experimental apparatus

The experimental apparatus employed to measure the power thresholds is based on an instrument previously developed [12] to compare the visual acuity in the visible spectrum with that provided by the 2P vision in the IR. Further details of the apparatus can be found in the reference. For the current experiment a different type of light source was added. It is a supercontinuum laser (SuperK COMPACT, NKT Photonics, Birkerød, Denmark) with a broadband spectrum from 450 nm to 2400 nm that emits pulses in the order of 1 ns at selectable repetition rates up to 20 kHz, with the pulse width and energy independent of the pulse repetition rate as stated by the laser manufacturer. After dispersion in the optical setup and ocular media, and due to the relatively long pulse width, the pulses are broadened by a negligible factor of roughly $(1 + 10^{-10})$ [13].

Figure 1 shows a schematic of the optical setup showing the relevant components for this experiment.

The output from the supercontinuum source is spectrally filtered by a bandpass filter. The set of filters available allowed us to select wavelengths at 850, 880, 900, 920, 950, 1000, 1050 and 1100 nm with a spectral bandwidth (FWHM) of 10 nm except the filters at the wavelength of 850 nm (FWHM=40 nm) and at 1050 nm (FWHM=50 nm). No measurements were performed beyond 1100 nm because water absorption in the eye made them impractical. To ensure that no visible light enters the system leaked from the bandpass filters, a longpass filter with cut-on wavelength at 800 nm is placed next providing a transmission below the cut-on wavelength that is 10^{-7} times the transmission above. In addition, transmission of all filters was measured using a spectrometer in the visible range (USB4000, Ocean Optics, Largo (FL). USA) finding no leaking that could potentially be misinterpreted as color vision in the IR. A shortpass dichroic mirror with cutoff wavelength at 650 nm reflects the IR light at the same time that allows visible light

Biomedical Optics EXPRESS

from a CW laser emitting at 543 nm to be coupled into the system. A variable aperture (A1 in the figure) after the dichroic mirror produces the entrance pupil of the optical setup. This aperture is optically conjugated by means of lenses L1 and L2 with a 2-axis galvo mirror system which in turns is conjugated with the eye's pupil plane by lenses L3 and L4. Proper control over the galvo mirrors allows us to scan the light beam onto the retina to deliver visual stimuli. As a safety measure and to control the duration of the luminous excitation the galvo mirrors can deflect the beam out of the aperture (A2) placed between lenses L3 and L4. The power reaching the eye's pupil can be attenuated by a variable neutral density filter which can be manually operated by the participant. In addition, trial lenses can be placed in front of the eye to provide the sharpest possible image on the retina.

The visual stimulus employed was a Tumbling E letter, the size of each bar (and the gap between them) subtending 2 minutes of arc. Total size of the letter is 10×10 arcmin. The galvo mirrors were driven to scan each point of the letter at a rate of 52.4 Hz high enough for the

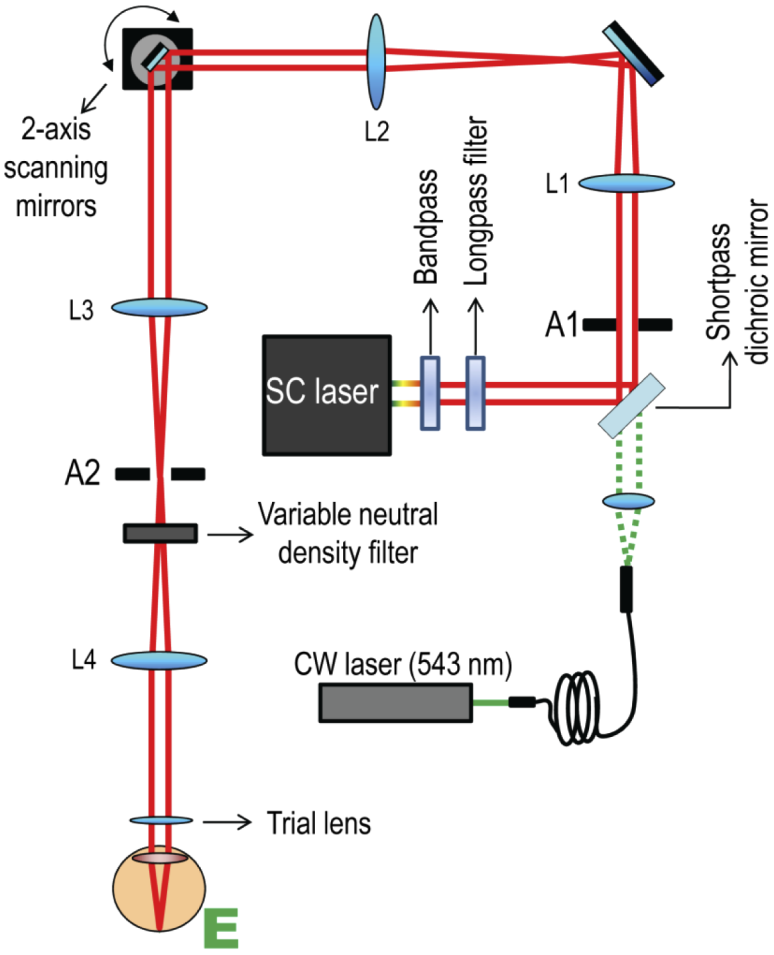

Fig. 1. Schematic diagram of the experimental apparatus. The beam from a supercontinuum laser is spectrally filtered by a bandpass and a longpass filters and scanned onto the retina by the 2-axis scanning mirrors. Apertures A1 and A2 are used to select the beam size and to block the beam when necessary respectively. An additional CW laser is available through a shortpass dichroic mirror. Trial lenses are used to correct for the eye's ametropias.

Biomedical Optics EXPRESS

participant not to perceive a flickering image. The refresh rate value was determined by using an oscilloscope (MDO3032 Tektronix Inc. Beaverton OR, USA), reading the voltage signal from a photodetector (PDA36A-EC, Thorlabs, Newton NJ, USA) placed in the way of the scanning beam. Although the size, shape and duration of visual stimuli have an influence on the minimum power needed for the stimulus to be detected [14], these factors are not critical in our experiment since our conclusions will be derived from power threshold comparisons rather than from absolute values.

2.2. Participants

A total of four volunteers, with ages ranging from 25 to 44, participated in the experiment. Two were emmetropes and the other two mild myopes with no astigmatism. All of them declared not to suffer ocular pathologies that could pose a risk for their ocular health or could affect the experimental outcome (color or sensitivity deficiencies). They all were members of the lab well trained in psychophysical experiments. The experiment followed the tenets of the declaration of Helsinki. Participants were informed of the nature of the experiment and the potential risks involved and signed a consent form.

2.3. Experimental procedure

Participants' pupils were initially aligned with the exit pupil of the apparatus using a bite bar to ensure the highest position stability. In those cases where it was needed the participant's refractive error was corrected by means of trial lenses. The background light in the laboratory was kept at the minimum by covering all light sources such as reflections from the supercontinuum laser, computer screens or light indicators of the electronic devices. Before starting the measurements, participants were dark adapted for 15 minutes under these conditions. In-between trials there was a pause of approximately 2 minutes during which the participants were asked to close his/her eyes to keep dark adaptation. The visual stimulus is continuously produced by the scanning system and participant's task consisted of manually rotating the variable neutral density filter to search for the minimum power that allows for stimulus detection or power threshold. Although this method of adjustment is not suitable for obtaining an absolute threshold, as in a probabilistic based method, it is itself valuable since the Bloch's law, on which part of this work is based, was established by measuring thresholds by means of a similar method. At the beginning of each trial the neutral density filter was always set at an angle that ensured that the visual stimulus would not be detected and then the participant was instructed to rotate the filter increasing the transmittance. Once around the power threshold the participant was free to change the luminous power to refine the assessment of the threshold. After each trial, a power meter was placed at the eye's pupil plane and the average power was measured. For each tested wavelength, the measurements of the power corresponding to 3 trials were averaged. The procedure was repeated for 2 different pulse repetition rates, 1.98 kHz and 9.91 kHz. These values were read off the console of the driver of the supercontinuum laser and initially checked using the photodetector and oscilloscope used to previously measure the refresh rate of the stimulus. The whole experimental procedure took around 2 hours.

For all tested wavelengths the exit pupil of the instrument was set at 1.5 mm and hence there was no need to use mydriatics to enlarge the participant's pupil. This reduced aperture provided a good quality visual stimulus, and at the same time prevented the focus error produced by the longitudinal chromatic aberration (LCA) from having a significant impact. Furthermore, by leaving the participant's accommodation free, we let the eye counteract the LCA by allowing the distant focus to move closer to the retina with longer wavelengths.

In this kind of experiments involving intense pulsed light sources, ocular safety must be considered carefully. We estimated [15,16] the maximum permissible exposure for our particular experimental conditions and in all cases power thresholds occur at powers which were far from

Biomedical Optics EXPRESS

these limits (the calculations to estimate the safety limits are described in detail in the appendix). However, the fact that the participant was given control over the light intensity through the variable neutral density filter requires additional safety measures. To ensure that hazardous limits were never reached the area of the neutral density filter with the highest transmittance was blocked in such a way that the exposure will always be below the safety limits no matter the angle the filter was set or the experimental condition (wavelength, pulse repetition rate) tested.

2.4. Theoretical model

We developed a simple theoretical model to predict the power thresholds measured at the different pulse repetition rates. With very weak stimuli, at the level of threshold detection, the visual system follows the Bloch's law [6,7]. It states that at the threshold detection, and for a certain period of time in the order of hundreds of milliseconds [17], the product of the luminance times the duration of the visual stimulus is constant. It basically means that the relevant magnitude is the total energy collected and in consequence shows the existence of a temporal integration in the visual system. The maximum duration of the visual stimulus where this law still holds is termed the temporal integration window. In other words, in order to detect a stimulus a minimum number of photons are required. In turn, this means that a minimum number of the molecules with chromophores contained in the light sensitive cells of the retina have to be activated (isomerized) in order to trigger a neural signal and all together produce a visual sensation. Bloch's law was experimentally proved using continuous light where only linear optics processes take place and indeed a deviation from this law is indication of the presence of a nonlinear effect [5]. Nonetheless the underlying idea of Bloch's law that a minimum number of light sensitive molecules have to be excited in order for a stimulus to be detected should still hold even in the presence of nonlinear effects. We used this assumption to derive an expression for the minimum average power that is needed to detect a visual stimulus assuming the involvement of either a 2P or a 1-photon (1P) process.

2.4.1. Assuming a 2P absorption process

To this end we basically followed the theoretical development by Xu et al. [18] carried out to estimate the 2P excitation cross-section of different fluorophores. In the first place and from a general point of view, the number (n_{2p}) of photons absorbed per unit time in a 2P process in a solution containing a concentration C of a certain absorbing molecule illuminated by light with intensity I, can be expressed as [19]

$$n_{2p} = \int_V C(\mathbf{r},t)\, I^2(\mathbf{r},t)\, \sigma_2 \, \mathrm{d}v \tag{1}$$

where V is the volume of the illuminated sample, $\boldsymbol{r}$ is the position vector, t represents time and σ_2 is the 2P absorption cross-section. Because, in this case, the absorption of 2 photons involves the activation of one single molecule, the number (n^*_{2p}) of molecules in the excited state per unit time, considering the quantum yield (ϕ) must be

$$n^*_{2p} = \phi \frac{1}{2} n_{2p} \tag{2}$$

The 2P absorption cross-section, σ_2, is constant in space. In addition, and assuming that there is no saturation, the concentration of available molecules to be excited is independent of time and $C(\mathbf{r},t)$ becomes $C(\mathbf{r})$. In the case of the retina, keeping the spatial dependence of the concentration allows us to reflect the localized distribution of these molecules only into the outer

Biomedical Optics EXPRESS

segments of the cone photoreceptors. With these considerations and taking Eq. (1) into Eq. (2)

$$n^*_{2p}=\frac{1}{2}\phi\,\sigma_2\int_V C(\mathbf{r})\,I^2(\mathbf{r},t)\;\mathrm{d}v \tag{3}$$

To simplify the integral on the right-hand side of the last equation we start by separating the temporal and spatial dependence of the intensity:

$$I(\mathbf{r},t)=\;I_0(t)\,S(\mathbf{r}) \tag{4}$$

where $I_0(t)$ is the intensity at the geometric focus and $S(\mathbf{r})$ is a unitless function. Equation (4) represents intensity as a constant relative spatial distribution changing over time as a whole accordingly to $I_0(t)$. This is a valid representation of any imaging system with fixed optical characteristics illuminated by a time dependent light source. Except for potential accommodation this model perfectly fits the case where the eye is illuminated by a pulsed light source. Equation (3) can then be rewritten as:

$$n^*_{2p}=\frac{1}{2}\phi\,\sigma_2\,I_0^2(t)\int_V C(\mathbf{r})\,S^2(\mathbf{r})\;\mathrm{d}v \tag{5}$$

On the other hand the intensity at the focal point and the instantaneous power $P(t)$ entering the optical system can be related by the next equation [18]:

$$I_0(t)=\frac{\pi(N.A.)^2}{\lambda_0^2}\;a\,P(t) \tag{6}$$

with $N.A.$ the numerical aperture of the optical system, λ_0 the wavelength in vacuum of the light irradiating the sample and a the transmittance of the media before the focal point. This parameter represents the absorption of light by the ocular media, mainly by water.

Equation (6) allows us to rewrite n^*_{2p} in terms of the instantaneous power:

$$n^*_{2p}=\frac{1}{2}\phi\,\sigma_2\,\pi^2\frac{(N.A.)^4}{\lambda_0^4}a^2\,P^2(t)\,S_2^{(o)} \tag{7}$$

where $S_2^{(o)}$ represents the integral in the right-hand side of Eq. (5). It contains the overall spatial dependence derived from both light spatial distribution and molecule concentration.

The total number (N^*_{2p}) of molecules excited in a certain finite period of time τ by a pulsed light source can then be easily calculated by integrating Eq. (7) assuming squared pulses with instantaneous peak power P_p, pulse width t_p and pulse repetition rate F:

$$N^*_{2p}\,(\tau)\;\;=\;\;\frac{1}{2}\;\phi\;\sigma_2\,\pi^2\;\frac{(N.A.)^4}{\lambda_0^4}\;a^2\,\tau\,F\;t_p\,P_p^2\,S_2^{(o)} \tag{8}$$

This can be expressed in terms of the average power by using the relationship $\langle P\rangle = P_p\,t_p\,F$

$$N^*_{2p}\,(\tau)\;\;=\;\;\frac{1}{2}\;\phi\;\sigma_2\,\pi^2\;\frac{(N.A.)^4}{\lambda_0^4}\;a^2\;\;\frac{\tau}{t_p\,F}\;\;S_2^{(o)}\langle P\rangle^2 \tag{9}$$

Now let N_{th} be the minimum number of opsin molecules in an excited state required to detect the stimulus during the temporal integration window τ. Then, at the threshold, $N^*_{2p}(\tau)=N_{th}$ and the corresponding average power can be solved from Eq. (9):

$$\langle P\rangle_{th}\;\;=\;\;\frac{\lambda_0^2}{\pi a\,(N.A.)^2}\;\sqrt{\frac{2\,t_pF}{\phi\,\sigma_2\,\tau\,S_2^{(o)}}N_{th}} \tag{10}$$

This average power can be identified with the power thresholds which are experimentally obtained from the participants. This equation does not allow us to calculate this magnitude

Biomedical Optics EXPRESS

because there are several variables with unknown values such as τ, C, σ_2, $S_2^{(o)}$ or N_{th} However, these values are the same independently of the pulse repetition rate and this allows us to predict that the ratio between power thresholds obtained at different repetition rates (F_1, F_2) must be:

$$\frac{\langle P\rangle_{th1}}{\langle P\rangle_{th2}} = \sqrt{\frac{F_1}{F_2}} \tag{11}$$

2.4.2. Assuming a 1P absorption process

For comparison, we derived an expression for the power thresholds assuming now a linear process where each molecule absorbs only 1 photon. In this case the equivalent to Eq. (1) is

$$n_{1p} = \int_V C(\mathbf{r},t)\, I(\mathbf{r},t)\, \sigma_1 \, \mathrm{d}v \tag{12}$$

where n_{1p} is the number of photons absorbed per unit time in a 1P process and σ_1 is the corresponding cross-section. Notice that in this case it must be $n_{1p}^* = \phi\, n_{1p}$. With these last equations as the starting point and following an identical development to that for 2P, an equivalent expression for the average power at the detection threshold can be found:

$$\langle P\rangle_{th} = \frac{\lambda_0^2}{\phi\, \sigma_1\, \pi\, (N.A.)^2\, a\, \tau S_1^{(o)}}\, N_{th} \tag{13}$$

where $S_1^{(o)} \equiv \int_V C(\mathbf{r})\, S(\mathbf{r})\, \mathrm{d}v$. Notice that in this case $\langle P\rangle_{th}$ does not depend on the pulse repetition rate and in consequence the ratio between power thresholds obtained at different repetition rates (F_1, F_2) is:

$$\frac{\langle P\rangle_{th1}}{\langle P\rangle_{th2}} = 1 \tag{14}$$

3. Results

Figure 2 shows the average across participants of the power thresholds as a function of wavelength for the two pulse repetition rates tested. Error bars stands for inter-participant variability. It can be noticed that in general error bars are larger in the shorter wavelength range from 850 to 900 nm. This may be explained by the additional difficulty to assess the threshold in this range because some sensitivity to normal vision still remains. This causes the initial perceived color to be a pale red produced by the L-cones. However, as the light intensity is increased the threshold for this color vision in the IR is surpassed and the S-cones start playing a role producing a blue color sensation. The simultaneous vision of red and blue produces a final perception of purple. And although the onset of purple is relatively abrupt there is an uncertainty range where the participant must decide whether the color is still red or purple. This purple color perception was reported earlier by Dmitriev et al. [9]. The power thresholds shown in Fig. 2 within this interval of wavelengths correspond to the detection of purple, that is, the threshold refers to the nonlinear phenomenon.

For the rest of wavelengths the corresponding colors perceived by the participants were, in general, described as follow: 920 nm (light blue); 950 nm (greenish light blue); 1000 nm (blueish light green); 1050 nm (green); 1100 (dark green).

Of special relevance for this work is the fact that the power thresholds for the higher pulse repetition rate are different to those for the lower repetition rate for all the tested wavelengths. The ratio, at each wavelength, of the power thresholds at 1.98 kHz with respect to those at 9.91 kHz is plotted in Fig. 3. It is fairly constant with an average value across wavelengths of 0.52

Biomedical Optics EXPRESS

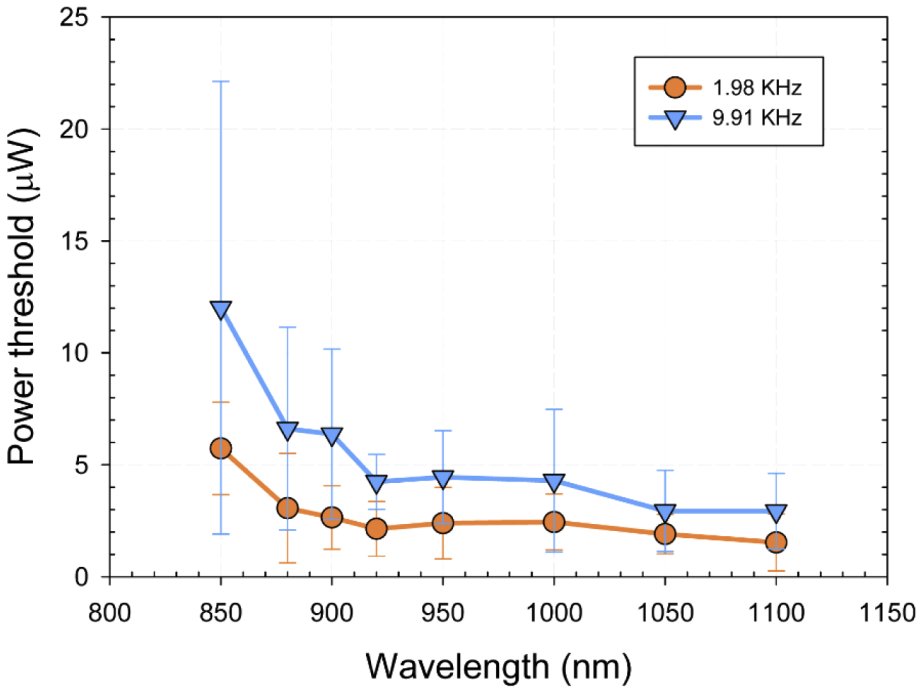

Fig. 2. Average across participants of the minimum average power needed to produce color vision in the IR, measured at selected wavelengths for 2 different pulse repetition rates. Error bars represent inter-participants variability (±1 standard deviation).

and standard deviation of 0.07. Along with these experimental data, in the same figure, the theoretical counterpart assuming a 2P and a 1P vision processes obtained from Eq. (11) and (14) respectively are also represented. For 2P the expected value is 0.45 and for 1P is 1.

Biomedical Optics EXPRESS

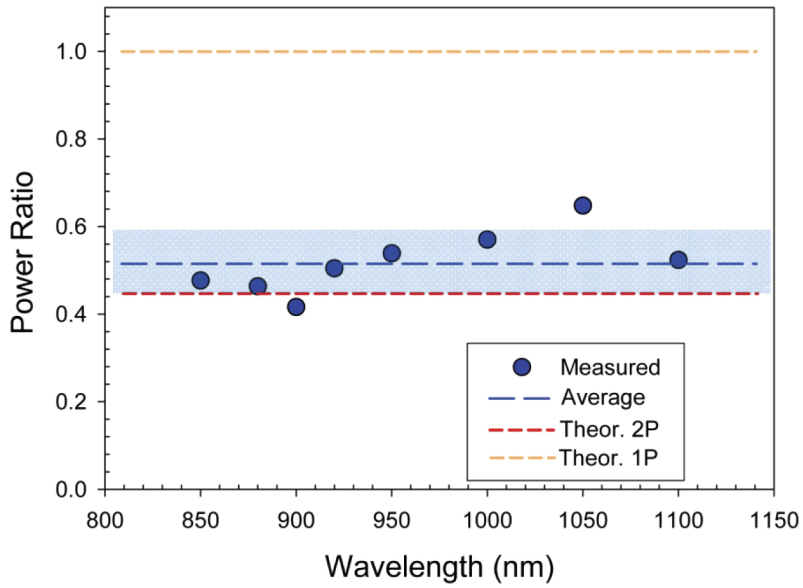

Fig. 3. Ratio of the average minimum power needed to perceive color in the IR measured at a pulse repetition rate of 1.98 kHz to that measured at 9.91 kHz. The average value is indicated by a dashed blue line. The blueish shaded area frames an interval of ±1 standard deviation. The expected values assuming either the involvement of 1 or 2 photons are indicated by the golden and red lines respectively.

4. Discussion

We have measured the power thresholds for the detection of pulsed IR as visible light at two different pulse repetition rates in a range of wavelengths in the IR. In addition, we have developed a theoretical model able to account for the experimental observations. In particular, this model predicts that the ratio between power thresholds at the 2 particular pulse repetition rates used in this experiment should be equal to 0.45 in case a 2P nonlinear process is involved and equal to 1 in case a 1P linear process is taking place. The experiment provided a relatively constant value across wavelengths of 0.52 ± 0.07. In consequence the comparison between expected and experimental values supports the theory that vision in IR is mediated by a nonlinear phenomenon involving 2 photons. Other authors in the past reached the same conclusion using different methods. We have employed a new approach based on the use of new light sources technology supported by a detailed theoretical model. That allowed us to provide a more comprehensive study of the nonlinear nature of this phenomenon.

A key element in our procedure is the estimation of light intensity thresholds, which are well known to be very sensitive to the previous luminous conditions the eye has been exposed. For this reason, at the beginning of the session, the participants stayed for 15 minutes with the eyes closed in absolute darkness until dark adaptation [20] is completed. The process of dark adaptation takes place independently for both light sensitive cells, rods and cones, and the 15-minutes period ensure rod adaptation. However, cone adaptation takes place in a much shorter period, in the order of 3-4 minutes [21] after exposure to ordinarily light intensities. Since our participants are detecting colors, it is actually their cones the cells involved. This is relevant because during each trial, the retina is exposed to a certain, although very low, light levels and consequently a cone related dark adaptation process is needed prior to the next trial. Since light exposure is around the detection threshold, much lower than ordinarily light intensities, the 2-minutes pause between trials during which the participant stayed with the eyes closed, ensured the eye was properly dark

Biomedical Optics EXPRESS

adapted. Moreover, we can discuss about light-adaptation that might be taken place during each trial because we left the participants to freely rotate the variable neutral density filter to refine their assessment of the threshold. In this sense we do not expect a significant influence because the cones recover very quickly to modest changes in steady ambient illumination. For example, it has been shown that circulating current in human cones can recover in about 100 ms after a large bleach [20].

In principle our study cannot be used to discriminate which one of the previously suggested nonlinear effects, 2P chromophore isomerization or SHG, is responsible for the vision in IR as visible light. The two main premises of the developed nonlinear model are met in both cases: the number of energized opsin molecules is proportional to the square of the luminous intensity and a couple of photons are needed to activate a single molecule. The last condition is met through different ways on each case although the final outcome is the same. In 2P chromophore isomerization the molecule is directly activated by 2 photons whilst for SHG the molecule is activated through an intermediate visible photon which in turn has been generated by 2 photons.

In order to obtain the equations of the theoretical model we assumed that there is no saturation and the concentration of available molecules to be excited is constant in time. This is justified because the experiment is performed at light intensities around the detection threshold level. Hence, no saturation is expected and the concentration of available opsin must be constant in time. Another assumption we made is that the integrals in Eq. (5) and (13), named as $S_2^{(o)}$ and $S_1^{(o)}$ respectively, have the same value independently of the pulse repetition rate. This, in turn, is supported by the idea that the light distribution in the focal point on the retina is unaltered with the pulse repetition rate. To test this hypothesis we recorded the PSF produced after a 300-mm focal length lens placed near the eye's pupil plane through the 1.5-mm pupil. These images are shown for our two tesded frequencies in Fig. 4 along with 2 horizontal intensity profiles to facilitate the comparison. The only difference in the optical setup, from the recording of one image at one frequency to the next, was a change in transmittance to equalize the maximum brightness between frequencies. Although the PSF is only a section of the volumetric light distribution near the focus, the almost perfect agreement between both PSFs strongly support our initial assumption.

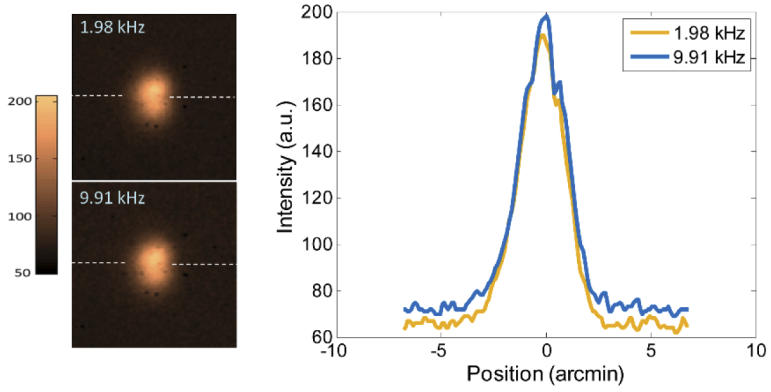

Fig. 4. Comparison of the PSFs recorded at the 2 different pulse repetition rates tested. Left: images of both PSFs. Right: Intensity profiles obtained from both PSFs along the dashed line superimposed on the PSFs images.

Another implicit assumption made is related with the way the visual stimulus is detected. The 2-arcmin E letter used as the stimulus is produced by scanning the focal spot point by point onto the retina. To consider that the detection of the E letter has to be done through the detection of each of these individual points would introduce significant complications in

Biomedical Optics EXPRESS

the theoretical calculations. For instance, in the calculation of the arriving photons during the temporal integration window onto a particular location on the retina we should have taken into account the coupling between the stimulus refresh rate and the pulse repetition rate. Because none of them are infinite there may be the case for certain locations on the retina that no pulses are delivered in one sweep of the scanners even when they are pointing to that location. Actually, the number of pulses delivered in one single sweep onto the whole area of the stimulus is 38 (2 kHz) and 191 (10 kHz) (the different number does not have an impact on the visual appearance of the stimulus). Instead, we have simplified this issue and assumed that the detection of the stimulus takes place as a whole and not point by point. The detection happens when N_{th}, the minimum number of opsin molecules in an excited state required to detect the stimulus within the temporal integration window, is reached on the total retinal area under the scanned E letter.

For completeness, it is of interest to discuss briefly about photoreversal. Once the opsin molecule absorbs a photon, it initiates a chain of events and transformations in different compounds that ultimately lead to the transduction in an electric signal. What Williams [22] and others found studying ex-vivo the rhodopsin contained in frog retinas was that these compounds can, in turn, absorb photons and become rhodopsin (photoreversal) increasing the concentration of this molecule. This is not an issue for the validity of our model: firstly because it has been shown that photoreversal does not happen in the human retina [23,24], and secondly because even if this effect occurred, this would only increase the concentration of opsin and would be in favour of the validity of the assumption.

The measurement of the power thresholds at several wavelengths showed that, even though they are significantly changing, specially at shorter wavelengths, however the ratios of these power thresholds at the different pulse repetition rates are relatively constant. This is in agreement with the theoretical model which predicts that these ratios should be independent of wavelength.

The spectral dependence of power thresholds was previously reported in different publications. It is very difficult to compare absolute values between studies because many other factors, such as stimulus size and shape, are different. Palczewska [10] measured the sensitivity (inverse of the power threshold) between 780 and 1150 nm and found that it was monotonically decreasing in a range of 5 orders of magnitude toward longer wavelengths. These results cannot be directly compared with ours, in particular in the shorter wavelength range between 780 and 900 nm where most of the variation takes place, because they included also normal vision in the IR through a normal linear process. For longer wavelengths they showed no clear tendency which roughly agrees with the fairly constant values we measured in this spectral range. Another publication reporting results on this topic was authored by Dmitriev et al. [9]. They measured the sensitivity with resolution below 5 nm and found a sort of oscillating behavior with high amplitude and with a bell shaped-like envelope peaking around 1120 nm. These unexpected results differ clearly from the smooth behavior we measured although the much higher sampling in wavelength in Dmitriev's study has to be considered. All of the above suggests that further research on the spectral sensitivity might shed light on these discrepancies and in general on nonlinear vision in the IR.

In summary, we performed a visual experiment with pulsed IR light which supports the theory that the basis of the phenomenon are nonlinear optical processes.

Appendix

A detailed description of the light safety calculations will be given in this appendix. They are based on the excellent paper by Delori et al. [15] adapting the guidelines provided by the ANSI standard to ophthalmic applications where the eye or head movements may be restrained, as it is the case in our experiment. We will consider the safety limits for the retina and the anterior segment (cornea and lens).

Biomedical Optics EXPRESS

A1. Retina

We are scanning the retina with a light beam that produces an E letter inscribed in a 10×10 arcmin square. In principle, the procedures devised to estimate safety limits for these scanning devices, such as SLO, should be followed. But our scanning system differs from that in a standard SLO in 2 main aspects: retinal field and scanning sequence. The scanned retinal field in a SLO may range from 1° to 50° and in our case is only a very small fraction of it, 10 arcmin. This only represents twice the size that is considered in the light safety related literature as the smallest spot size (α_{min}=1.5 mrad). Regarding the scanning sequence, in a SLO there is a fast and a slow scanning mirror which in practice scan the retina based on line segments. This fact is used to estimate safety limits, as in example E of Delori's paper. The two mirrors that compose our scanning system move at the same speed and hence the idea of a line segment scan is not applicable. The above considerations move us to think that might not be safe to make use of previously reported calculations for standard SLOs. A very restrictive approach, given the reduced scanned area, would be to consider the stimulus as a point-like image and that the retina was illuminated with what is termed a small source (α=a_{min}). But this not realistic either because the focus is actually being scanned and that contributes to relax the safety limits. As a compromise, we finally decided to consider that the retina was illuminated with a steady beam and an extended source the size of the E letter.

An additional consideration that must be made is that ANSI standards are defined for circular images on the retina. The E letter is far from that and corrections must be applied if we want an extra level of precision in our calculations. These corrections can be found in Table 4 of Delori's paper for square areas. The E letter, although inscribed into a square, has non illuminated areas between the bars. We have approached the real shape of the E considering it as a square with the same area than the actual E. This means that the new effective size of the squared stimulus must be affected by a 0.82 factor and the new size to consider is α=0.82×10 arcmin = 8.2 arcmin. Now, following section 6. D and Eq. (11) and (12) in Delori's paper, the maximum permissible power (MPΦ) for our extended squared source can be calculated as

$$MP\Phi \;=\; MP\Phi_{small\ source}\, C'_E \tag{15}$$

where (Table 4)

$$C'_E = \frac{4\alpha}{\pi\, \alpha_{\min}} \tag{16}$$

and $MP\Phi_{small\ source}$ is the maximum permissible power for a source with size α_{min}. Taking into account the new value for α, the factor C'_E its then equal to 2.0. This means that we need to calculate the MPΦ as if the stimulus were a small source and then multiply it by the size related correcting factor C'_E.

To estimate $MP\Phi_{small\ source}$, we have to consider that we are exposing the eye to repetitive pulses and section 7 of the Delori's paper must be used. To determine what is the maximum permissible average power in this case, three rules must be followed and the one providing the most restrictive exposure must be chosen. To facilitate this step, Table 5 limits these options depending on pulse duration (t_p) and pulse repetition rate or frequency (F). In our case, on the one hand, t_p is in the order of 1 ns and always smaller than the parameter t_{min} (18 or 50 μs, depending on wavelength). On the other hand, F (~2 or 10 kHz) is less than the critical frequency parameter (F_{cr} = 1/ t_{min}). This means that the 2 rules included in cell b of table 5 should be tested. The first of these rules to test is rule 2 (average power limit) related with photochemical damage which is applicable only in the wavelengths range between 400 and 600 nm. This can be immediately discarded because we used IR light. The last of these rules is rule 3 (multiple pulse limit) and must be evaluated assuming that t_p=t_{min}. The application of this rule yields, accordingly to

Biomedical Optics EXPRESS

Tables 3 and 5 in Delori's paper, the next expression for the maximum permissible average power:

$$MP\Phi_{small\ source} = F^{0.75}\, T^{-0.25}\, t_{\min}\, 1.07x10^{2}\, C_T C_J\, C_E \tag{17}$$

where T is the total exposure duration and C_T, C_J and C_E are parameters which can be found in Table 2 of Delori's paper. Their values for each wavelength have been obtained and are listed in Table 1. We have been very conservative when estimating the value of T. Although each trial took in average about 30 seconds which was followed by a 2-minutes pause, we have preferred to consider T as the sum of the duration of all the trials. Then, T= (8 wavel.) x (2 Freq.) x (3 trials) x 30 s = 1440 s.

Table 1. values of the parameters in Eq. (17)

Wavelength (nm)	t_{min}(μs)	C_T	C_J	C_E
850	18	2.0	1	1
880	18	2.3	1	1
900	18	2.5	1	1
920	18	2.8	1	1
950	18	3.2	1	1
1000	18	4.0	1	1
1050	18	5.0	1	1
1100	50	5.0	2	1

Now, combining our Eq. (15) and (17), we obtain the final expression for the average MPΦ:

$$MP\Phi_{av} = 2.0\ F^{0.75}\, T^{-0.25}\, t_{\min}\, 1.07x10^{2}\, C_T C_J\, C_E \tag{18}$$

Using this last equation, we have plotted (Fig. 5) and compared the $MP\Phi_{av}$ with the measured power thresholds.

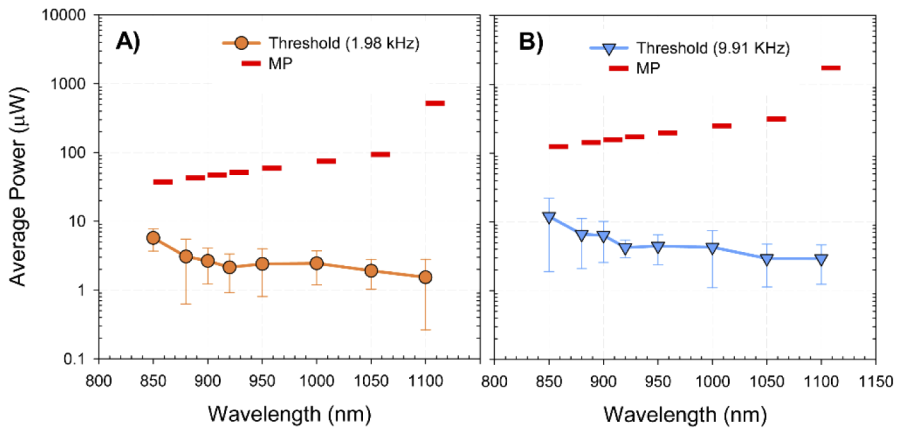

Fig. 5. Comparison of the maximum permissible (MP) average power with the measured average power for the thresholds at the two tested frequencies, A) 1.98 kHz and B) 9.91 kHz.

In addition, we have also made a similar comparison for the peak power (P_p) using the data contained in Fig. 5 and making use of the next expression relating average with peak power: $P_p = \langle P \rangle / (t_p F)$. The results are graphed in Fig. 6.

Biomedical Optics EXPRESS

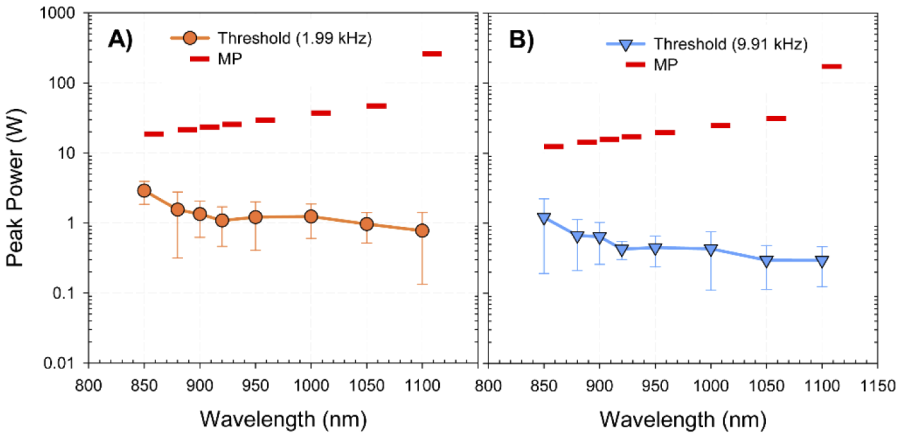

Fig. 6. Comparison of the maximum permissible (MP) peak power with the measured peak power for the thresholds at the two tested frequencies, A) 1.98 kHz and B) 9.91 kHz.

A2. Cornea and lens

Under the particular conditions of our experiment, using IR light in the range from 850 nm to 1100 nm, it is considered that no additional precautions are needed to protect the anterior segment of the eye as long as the retina is not exposed to harmful light levels. However, after the revision of the ANSI standards in 2014, the retinal exposure limits were increased in the wavelength range between 1250 nm to 1400 nm and that may pose a risk for the anterior segment, as it is described in this work by Schulmeister et al. in 2019 [25]. Nevertheless, no IR light within this range was employed in this experiment, making it no necessary to include explicit calculations for the safety of the anterior segment.

Funding

Agencia Estatal de Investigación (PID2019-105684RB-I00); Fundación Séneca (19897/GERM/15).

Acknowledgments

We thank Juan M. Bueno for comments on the theoretical model. D. Sola thanks the PIT2 program of the University of Murcia.

Disclosures

The authors declare no conflicts of interest.

References

1. Commission Internationale de l'Éclairage (Cambridge University Press, 1924).
2. C. F. Goodeve, "Relative Luminosity in the Extreme Red," Proc. Roy. Soc. A **155**, 664–683 (1936).
3. D. R. Griffin, R. Hubbard, and G. Wald, "The Sensitivity of the Human Eye to Infra-Red Radiation," J. Opt. Soc. Am. **37**(7), 546 (1947).
4. L. S. Vasilenko, V. P. Chebotaev, and Y. V. Troitskii, "Visual observation of infrared laser emission," Sov. Phys. JETP **21**, 513–514 (1965).
5. D. H. Sliney, R. T. Wangemann, J. K. Franks, and M. L. Wolbarsht, "Visual sensitivity of the eye to infrared laser radiation," J. Opt. Soc. Am. **66**(4), 339–341 (1976).
6. M. A. Bloch, "Expériences sur la vision," Comptes Rendus la Soc. Biol. **37**, 493–495 (1885).
7. A. Gorea, "A refresher of the original Bloch's law paper (Bloch, July 1885)," i-Perception **6**(4), 1–6 (2015).
8. Q. Zaidi and J. Pokorny, "Appearance of pulsed infrared light: second harmonic generation in the eye," Appl. Opt. **27**(6), 1064–1068 (1988).

Biomedical Optics EXPRESS

9. V. G. Dmitriev, V. N. Emel'yanov, M. A. Kashintsev, V. V. Kulikov, A. A. Solov'ev, M. F. Stel'makh, and O. B. Cherednichenko, "Nonlinear perception of infrared radiation in the 800–1355 nm range with human eye," Quantum Electron. **9**(4), 475–479 (1979).
10. G. Palczewska, F. Vinberg, P. Stremplewski, M. P. Bircher, D. Salom, K. Komar, Z. Jianye, M. Cascella, M. Wojtkowski, V. Kefalov, and K. Palczewski, "Human infrared vision is triggered by two-photon chromophore isomerization," Proc. Natl. Acad. Sci. U. S. A. **111**(50), E5445–E5454 (2014).
11. D. Ruminski, G. Palczewska, M. Nowakowski, A. Zielińska, V. J. Kefalov, K. Komar, K. Palczewski, M. Wojtkowski, K. Komar, K. Komar, K. Palczewski, K. Palczewski, K. Palczewski, M. Wojtkowski, M. Wojtkowski, and M. Wojtkowski, "Two-photon microperimetry: sensitivity of human photoreceptors to infrared light," Biomed. Opt. Express **10**(9), 4551 (2019).
12. P. Artal, S. Manzanera, K. Komar, A. Gambín-Regadera, and M. Wojtkowski, "Visual acuity in two-photon infrared vision," Optica **4**(12), 1488–1491 (2017).
13. G. McConnell, "Improving the penetration depth in multiphoton excitation laser scanning microscopy," J. Biomed. Opt. **11**(5), 054020 (2006).
14. S. Hecht, S. Shlaer, and M. H. Pirenne, "Energy, quanta and vision," J. Gen. Physiol. **25**(6), 819–840 (1942).
15. F. C. Delori, R. H. Webb, and D. H. Sliney, "Maximum permissible exposures for ocular safety (ANSI 2000), with emphasis on ophthalmic devices," J. Opt. Soc. Am. A **24**(5), 1250–1265 (2007).
16. *ANSI Z136.1-2014* (Laser Institute of America, 2014).
17. H. B. Barlow, "Temporal and Spatial Summation in Human Vision at Different Background Intensities," J. Physiol. **141**(2), 337–350 (1958).
18. C. Xu and W. W. Webb, "Measurement of two-photon excitation cross sections of molecular fluorophores with data from 690 to 1050 nm," J. Opt. Soc. Am. B **13**(3), 481 (1996).
19. W. M. McClain and R. A. Harris, "Two-photon molecular spectroscopy in liquids and gases in Excited States," in *Excited States*, E. C. Lim, ed. (Academic, 1977), pp. 1–56.
20. T. Reuter, "Fifty years of dark adaptation 1961-2011," Vision Res. **51**(21-22), 2243–2262 (2011).
21. S. Hecht, C. Haig, and A. M. Chase, "The influence of light adaptation on subsequent dark adaptation of the eye," J. Gen. Physiol. **20**(6), 831 (1937).
22. T. P. Williams, "Photoreversal of rhodopsin bleaching," J. Gen. Physiol. **47**(4), 679–689 (1964).
23. H. Ripps and R. A. Weale, "Flash bleaching of rhodopsin in the human retina," J. Physiol. **200**(1), 151–159 (1969).
24. T. D. Lamb, "Evolution of vertebrate retinal photoreception," Philos. Trans. R. Soc., B **364**(1531), 2911–2924 (2009).
25. K. Schulmeister, M. Jean, D. Lund, and B. E. Stuck, "Comparison of corneal injury thresholds with laser safety limits," in *International Laser Safety Conference* (Laser Institute of America, 2019), Vol. 303, p. 303.